

Metrological Characterization of the Bunch Length System Measurement of the ELI - NP Electron Linac

L. Sabato^{1,2}, *D. Alesini*³, *P. Arpaia*⁴, *A. Giribono*⁵, *A. Liccardo*⁴, *A. Mostacci*⁵, *L. Palumbo*⁵, *C. Vaccarezza*³, *A. Variola*³

¹ Dept. of Engineering, University of Sannio, Corso Giuseppe Garibaldi, 107, 82100 Benevento, Italy. E-mail: luca.sabato@unisannio.it

² Istituto Nazionale di Fisica Nucleare (INFN) Naples, Complesso Universitario di Monte Sant'Angelo, via Cintia, Naples, Italy. E-mail: luca.sabato@na.infn.it

³ Istituto Nazionale di Fisica Nucleare (INFN/LNF) Laboratori Nazionali di Frascati, via Enrico Fermi, 40, 00044 Frascati, Italy

⁴ Dept. of Electrical Engineering and Information Technology, University of Naples Federico II, Via Claudio 21, Naples, Italy. E-mail: pasquale.arpaia@unina.it, annalisa.liccardo@unina.it

⁵ Dept. Scienze di Base e Applicate per l'Ingegneria (SBAI), University of Rome La Sapienza, Via Antonio Scarpa, 14, Rome, Italy

Abstract - Bunch length measurement in linac can be carried out using a Radio Frequency Deflector (RFD). A RFD provides a transverse kick to the beam introducing a correlation between the longitudinal coordinate of the bunch and the transverse coordinates, vertical or horizontal. So, through transverse beam size measurement on a screen, placed after the RFD, the bunch length can be obtained. In this paper, the metrological characterization of the bunch length measurement technique is proposed. The uncertainty and the systematic errors are estimated by means of a sensitivity analysis performed on the measurement parameters. The proposed approach has been validated through simulation by means of ELEGANT code on the parameters interesting for the electron linac of the Compton source at the Extreme Light Infrastructure - Nuclear Physics (ELI-NP).

Keywords: bunch length measurement, RF deflector, metrological characterization, sensitivity analysis, linear electron accelerator.

1. INTRODUCTION

ELI is an European project for high-level research on ultra-high intensity laser, laser-matter interaction and secondary sources. It will comprise four pillars: High Energy Beam Science in Prague (Czech Republic), Attosecond Laser Science in Szeged (Hungary), Laser-based Nuclear Physics in Magurele, near Bucharest (Romania), and Ultra High Field Science [1].

The Gamma Beam Source (GBS) at ELI-NP is going to focus on laser-based nuclear physics. While atomic processes are well suited to the visible or near visible laser radiation, as a third pillar ELI-NP will generate radiation and particle beams of higher energy and with brilliance suited to studies of nuclear and fundamental processes. This

infrastructure will cover a broad range of science: frontier fundamental physics, new nuclear physics and astrophysics as well as applications in nuclear materials, radioactive waste management, material science and life sciences [1]. This infrastructure will be an advanced Source of up to 20 MeV Gamma Rays based on Compton back-scattering, i.e. collision of an intense high power laser beam and a high brightness electron beam with maximum kinetic energy of about 720 MeV [2].

For a room temperature RF linac running at maximum repetition rate of about 100 Hz [3], the specifications on the requested spectral density cannot be achieved with single bunch collisions (i.e. one electron bunch per RF pulse colliding with one laser pulse). So, a RF linac design with capability to provide trains of bunches in each RF pulse, spaced by the same time interval needed to recirculate the laser pulse in a properly conceived and designed laser recirculator, has to be considered, in order to allow the same laser pulse to collide with all the electron bunches in the RF pulse, before being dumped. The final optimization foresees trains of 32 electron bunches separated by 16 ns, distributed along a 0.5 μ s RF pulse, with a repetition rate of 100 Hz. Every bunch has a length of about 1 ps [2].

High performance diagnostic is mandatory in order to achieve high brightness in high repetition rate machine. Important tasks are to measure the properties of the single bunch and the whole train of bunches [4–6]. Bunch length measurement can be carried out through a disruptive optical technique based on a RFD. The idea of this measurement technique is an old one and it has been used for bunch length measurements at Stanford Linear Accelerator Center (SLAC) free electron laser [7–9] and at SPARC-LAB linac [10–12].

In this paper, the simulation results of preliminary steps for a metrological characterization are presented. The tracking of the particles in the GBS electron linac are carried out by means of ELEGANT code [13, 14]. In section 2, the basic idea, the working principle and the procedure

of the bunch length measurement technique are presented. In particular, this measurement technique is based on the transverse beam dynamics theory that is explained in detail. In section 3, the simulation results are showed. In this section, the result of a bunch length virtual measurement at GBS electron linac is reported for the RFD phase $\varphi = 0^\circ$, using ELEGANT code [13, 14] and through the actual measurement procedure. The bunch length virtual measurement result for the RFD phase $\varphi = 180^\circ$ is reported in [15]. In section 3, the comparison between simulation and theoretical results of vertical bunch centroid and divergence average at screen are showed. Furthermore, the goodness of the approximation in the evaluation of calibration factor is reported. These results are carried out varying RFD phase between -30° and 30° , and -150° and 210° .

2. MEASUREMENT SYSTEM

In this section, the basic idea and the working principle of this measurement technique is presented. Moreover, uncertainty sources and systematic errors are introduced. This measurement technique is based on the transverse beam dynamics theory (subsection C). In the last subsection, the measurement procedure is treated.

A. Working Principle

Different types of measurements can be done with a RFD. Bunch length measurements can be done using only a RFD and a screen. Adding a magnetic dipole, the longitudinal emittance can be also measured [16]. The basic idea of these measurements is based on the property of the RFD transverse voltage to introduce a correlation between the longitudinal coordinate of the bunch and the transverse coordinates, vertical or horizontal, at the screen position [10, 11].

In bunch length measurements, the voltage phase is chosen in order to have a zero crossing of the transverse voltage in the center of the bunch, giving a linear transverse deflection from the head and the tail of the bunch itself. After the RFD, the transverse kick gives a transverse displacement of each longitudinal bunch slice, proportional to its position with respect to the bunch center [17]. Therefore, the information on bunch length can be derived from spot size measurements at screen, placed after the RFD [7–11].

B. Uncertainty Sources and Systematic Errors

In the GBS electron linac, the bunch length measurement system consists of a quadrupole, a RFD, a Beam Position Monitor (BPM) with correct magnet, a dipole, and a screen (see Fig. 1) [2]. The principal uncertainty sources and systematic errors of this measurement system are pointed out in Fig. 1. Bunch characteristics, device misalignments δ_i in respect of accelerator axis, tilt angles θ_i , and lengths L_i can affect the bunch length measurement. Moreover, the presence of magnets implies the presence of residual magnetic field B_i . Another point to investigate is the effect of quadrupole and

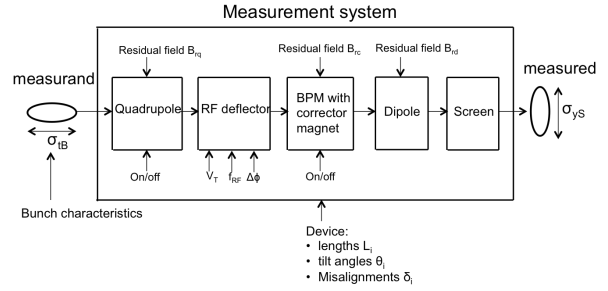


Fig. 1. Bunch length measurement system with uncertainty sources and systematic errors for GBS electron linac.

corrector magnet on the measurement. The parameters of RFD can also alter the bunch length measurement, but in principle some of their effects could be reduced using self-calibrate measurements (see subsection C). The effect of the screen is considered negligible.

C. Transverse Beam Dynamics

When the RFD is switched off (i.e. between RFD and screen there is a simple drift), the particle vertical divergence does not change and the particle vertical position changes. In particular, a particle, that starts at RFD center with a vertical position y_0 and a vertical divergence y'_0 , arrives at screen with vertical position $y_{s,off}$ and divergence $y'_{s,off}$ [18, 19]:

$$\begin{cases} y_{s,off} = Ly'_0 + y_0 \\ y'_{s,off} = y'_0 \end{cases}, \quad (1)$$

where L is the distance between the RFD center and screen. Assuming $\langle y_0 \rangle = 0$ m and $\langle y'_0 \rangle = 0^\circ$, the rms vertical spot size at screen is:

$$\sigma_{y_{s,off}}^2 = \sigma_{y_0}^2 + 2L\langle y_0 y'_0 \rangle + L^2 \sigma_{y'_0}^2, \quad (2)$$

where $\langle y_0 y'_0 \rangle$ is the correlation between vertical particle positions and divergences before RFD, σ_{y_0} and $\sigma_{y'_0}$ are the rms vertical distribution of particle positions and divergences before RFD, respectively. In bunch length measurement, the correlation term is not negligible, because the measurement system is designed in order to minimize the rms vertical spot size at screen with deflector off. Smaller $\sigma_{y_{s,off}}^2$ means better resolution, for amplitude deflecting voltage fixed. In order to achieve this goal, vertical focusing quadrupoles are used before RFD.

When the RFD is switched on, the particles feel a deflecting voltage when they pass through the RFD. The effect on every particle is a change in vertical divergence (see Fig. 2) [18–20]. We can assume the RFD voltage is:

$$V(z_0) = V_t \sin(kz_0 + \varphi), \quad (3)$$

where z_0 is the position of the particles along the beam axis with the origin in the RFD, $k = 2\pi/\lambda_{RF}$, λ_{RF} , V_t , and φ are the deflecting voltage wavelength, amplitude, and phase, respectively. Usually the bunch length is much smaller than

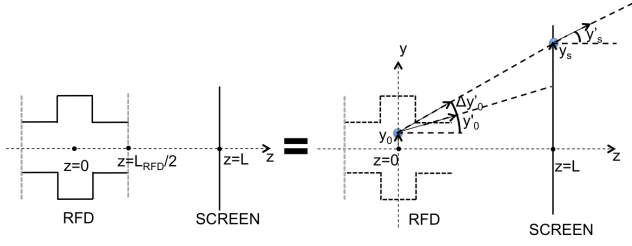


Fig. 2. Particle position and divergence at RFD center and at screen after the particle pass through a RFD. The particle is depicted in blue points (at the center of RFD and at screen).

RF wavelength (i.e. $kz_0 \ll 1$) and so we can use the following approximation [8, 9, 16]:

$$V(z_0) \approx V_t [kz_0 \cos(\varphi) + \sin(\varphi)]. \quad (4)$$

Therefore, RFD gives a vertical divergence change:

$$\Delta y'_0(z_0) = C_{rfd} [kz_0 \cos(\varphi) + \sin(\varphi)], \quad (5)$$

where $C_{rfd} = qV_t/(pc)$, q is the electron charge, p is the particle momentum, and c is the speed of light [8, 16]. Therefore, A particle arrives at screen with vertical position y_s and divergence y'_s :

$$\begin{cases} y_s = y_0 + L(y'_0 + \Delta y'_0), \\ y'_s = y'_0 + \Delta y'_0 \end{cases} \quad (6)$$

Equation (6) describes how vertical position and divergence change for every particle. If we consider a particle bunch, we need to consider the first and the second order momenta of the particle bunch (i.e. average and variance). Assuming $\langle z_0 \rangle = 0$ m, the vertical bunch centroid at screen is [8]:

$$C_{y_s} = LC_{rfd} \sin(\varphi), \quad (7)$$

the vertical divergence average is:

$$\langle y'_s \rangle = C_{rfd} \sin(\varphi), \quad (8)$$

and the rms vertical spot size at screen is [8]:

$$\sigma_{y_s}^2 = \sigma_{y_s,off}^2 + K_{cal}^2 \sigma_{t_0}^2, \quad (9)$$

where $\sigma_{y_s,off}$ is the rms vertical spot size at the screen with RFD off (2), σ_{t_0} is the rms bunch length (in seconds), $\langle y_0 z_0 \rangle$ and $\langle y'_0 z_0 \rangle$ are the correlations between particle longitudinal position and vertical position and divergence, respectively, and K_{cal} is a calibration factor:

$$K_{cal} = \omega_{RF} LC_{rfd} \cos(\varphi), \quad (10)$$

where ω_{RF} is the deflecting voltage angular frequency.

The rms vertical divergence distribution at screen is:

$$\sigma_{y'_s}^2 = \sigma_{y'_0}^2 + \left(\frac{K_{cal}}{L}\right)^2 \sigma_{t_0}^2. \quad (11)$$

Calibration Factor

The calibration factor is a coefficient that relates the vertical coordinate at the screen with the bunch longitudinal time coordinate. Comparing (7) and (10), an important relation can be noticed:

$$K_{cal} = \omega_{RF} \frac{dC_{y_s}}{d\varphi} \approx \omega_{RF} p, \quad (12)$$

where p is the slope of the plot vertical bunch centroid versus RFD phase, calculated by means a linear fit of vertical bunch centroid measurements for different RFD phase values. Equation (12) means that the coefficient K_{cal} can be directly calculated measuring the bunch centroid position at screen for different values of the RFD phase, i.e. it is possible to self-calibrate the measurements [17]. This is an important characteristic of this measurement technique.

D. Measurement Procedure

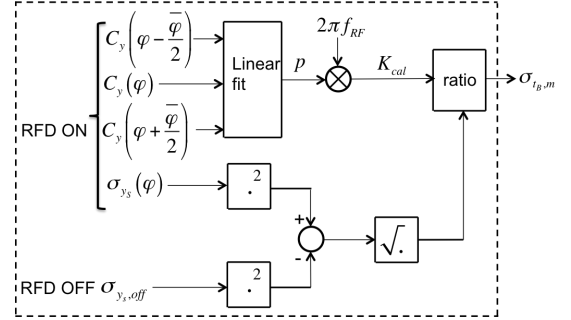


Fig. 3. Bunch length measurement procedure.

The proposed bunch length measurement procedure is divided in four steps (Fig. 3):

- first step: measurement of the rms vertical spot size at the screen with RFD off, $\sigma_{y_s,off}$;
- second step: measurements of vertical bunch centroid for different values of RFD phase with RFD on and from them by means of a linear fit the calibration factor, K_{cal} (12);
- third step: measurement of the rms vertical spot size at the screen with RFD on, σ_{y_s} ;
- fourth step: bunch length measurement $\sigma_{t_0,m}$, using the information of the previous steps and from (9):

$$\sigma_{t_0,m} = \frac{\sqrt{\sigma_{y_s}^2 - \sigma_{y_s,off}^2}}{|K_{cal}|}. \quad (13)$$

3. SIMULATION RESULTS

In this section, the result of a bunch length virtual measurement at GBS electron linac is reported for the RFD phase $\varphi = 0^\circ$, using ELEGANT code [13, 14] and through

the actual measurement procedure. The bunch length virtual measurement result for the RFD phase $\varphi = 180^\circ$ is reported in [15]. In this section, the comparison between simulation and theoretical results of vertical bunch centroid (7) and divergence average (8) at screen are showed. Furthermore, the goodness of the approximation (12) in the evaluation of calibration factor is reported. These results are carried out varying RFD phase between -30° and 30° , and -150° and 210° .

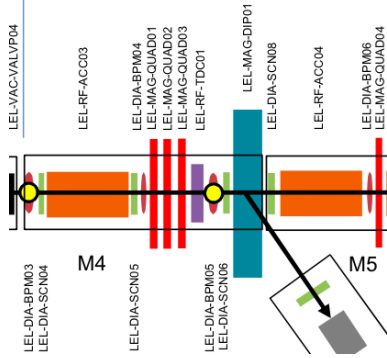


Fig. 4. Zoom of GBS linac layout between the first and the second C-band accelerating section [2].

Table 1. GBS electron linac bunch parameters (E is the bunch energy)

| σ_{y_0} [mm] | $\sigma_{y'_0}$ [μ rad] | $\langle y_0 y'_0 \rangle$ [m·rad] | σ_{t_0} [ps] | E [MeV] |
|---------------------|------------------------------|------------------------------------|---------------------|-----------|
| 0.3464 | 57.57 | $-1.986 \cdot 10^{-8}$ | 0.9117 | 118 |

Table 2. GBS electron linac bunch parameters

| V_t [MV] | f_{RF} [GHz] | ω_{RF} [Grad/s] | L [m] |
|------------|----------------|------------------------|---------|
| 1 | 2.856 | 17.94 | 1.1380 |

A nominal beam represented by 50000 particles has been tracked with ELEGANT code from LEL-RF-TDC01 RFD to LEL-DIA-SCN08 screen (Fig. 4), placed between the first and second C-band accelerating section of GBS electron linac [2]. The GBS electron linac bunch and RFD parameters are reported in Tabs. 1 and 2, respectively. The distance between RFD and screen $L=1.1380$ m.

A. Virtual Bunch Length Measurement

- First step: the virtual measurement of the rms vertical spot size at screen with RFD off is 0.281 mm. In the case of GBS linac bunches, the second term of (2), that takes in account the correlation between particle vertical divergences and positions cannot be neglected, because GBS linac bunches are focusing between the first and the second C-band accelerating section [15]. The rms vertical spot size at screen with RFD off does not depend on RFD parameters (see (2)).

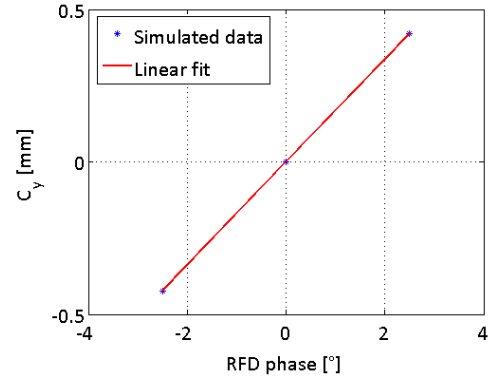


Fig. 5. Simulated data and linear fit of bunch centroid at screen used for the calculation of K_{cal} (12).

- Second step: the RFD phase is: $\varphi = 0^\circ$. C_{y_s} has been measured in three different values of RFD phase: $-2.5^\circ, 0^\circ$, and 2.5° (see Fig. 5). Using (12), the calibration factor can be evaluated with a relative error about 0.04 % from the theoretical value (10), i.e. $K_{cal} = 0.1737$ mm/ps.
- Third step: the virtual measurement of the rms vertical spot size at screen with RFD on and $\varphi = 0^\circ$ is 0.3226 mm.
- Fourth step: the bunch length virtual measurement can be assessed by means of (13) with a relative error less than 0.2 %.

The bunch length virtual measurement relative error for $\varphi = 180^\circ$ ([15]) is smaller than the relative error for $\varphi = 0^\circ$.

B. Varying RFD Phase

In the first part of the following simulations RFD phase is chosen between -30° and 30° with a step of 2.5° . In the second part of the following simulations RFD phase is chosen between -150° and 210° with a step of 2.5° .

RFD Phase centered in 0°

In Figs. 6 and 7, the vertical bunch centroid and the vertical divergence average at screen versus RFD phase are plotted (in blue * simulated data and in red line theoretical values (7) and (8)), respectively. Figs. 6 and 7 show a good match between theoretical and simulated results.

In Fig. 8, the relative error between theoretical (10) and approximated (12) calibration factor in function of RFD phase is showed. The maximum relative error between theoretical and approximated calibration factor is less than 0.07 %.

RFD Phase centered in 180°

In Figs. 9 and 10 the vertical bunch centroid and the vertical divergence average at screen versus RFD phase are plotted (in blue * simulated data and in red line theoretical

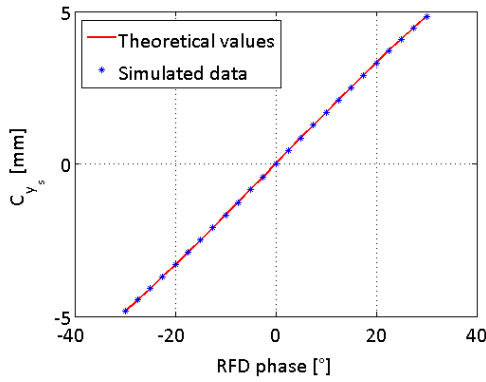


Fig. 6. Vertical bunch centroid at screen versus RFD phase. In blue * simulated data and in red line theoretical values 7.

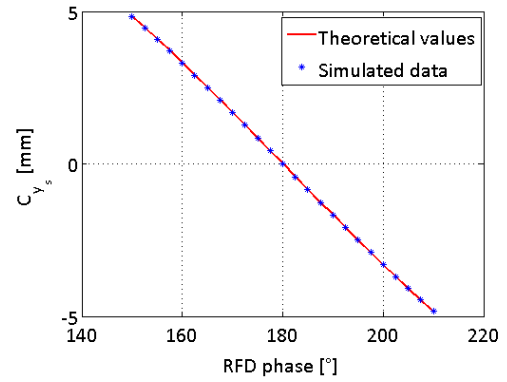


Fig. 9. Vertical bunch centroid at screen versus RFD phase. In blue * simulated data and in red line theoretical values 7.

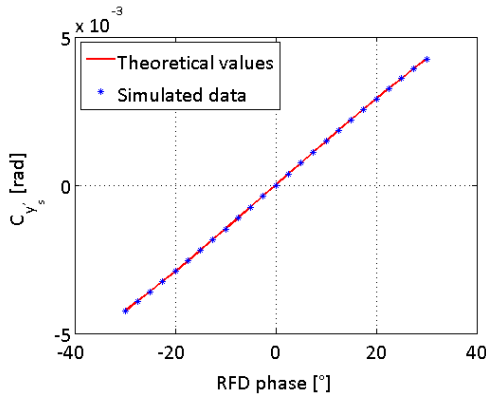


Fig. 7. Vertical divergence average at screen versus RFD phase. In blue * simulated data and in red line theoretical values (8).

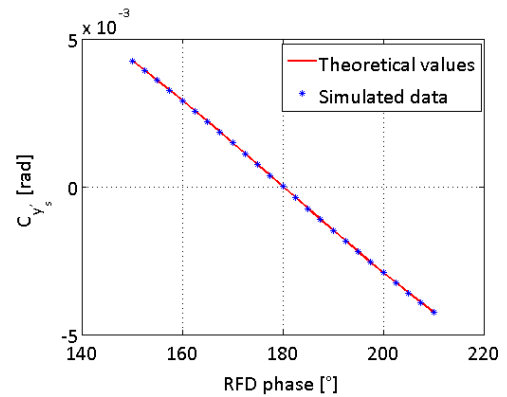


Fig. 10. Vertical divergence average at screen versus RFD phase. In blue * simulated data and in red line theoretical values (8).

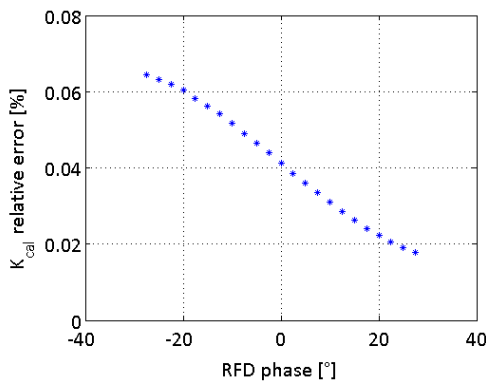


Fig. 8. Calibration factor relative error between theoretical (10) and approximated (12) versus RFD phase.

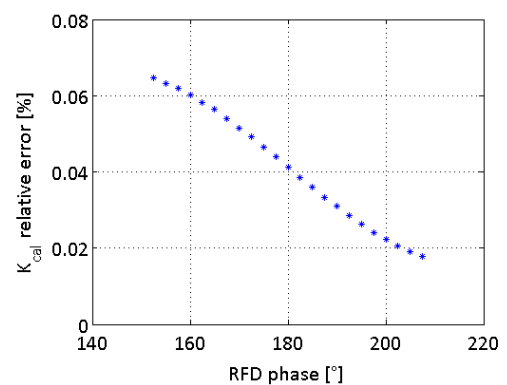


Fig. 11. Calibration factor relative error between theoretical (10) and approximated (12) versus RFD phase.

values). Figs. 6 and 10 show a good match between theoretical and simulated results. The slope of the plots in Figs. 6 and 9 has the same value but it changes only in sign.

In Fig. 11 the relative error between theoretical (10) and approximated (12) calibration factor in function of RFD

phase is showed. The maximum relative error between theoretical and approximated calibration factor is less than 0.07%. This result is equal to the case in which RFD phase is centered at 0°.

4. CONCLUSIONS AND FUTURE DEVELOPMENT

In this paper, the actual bunch length measurement procedure has been presented and it has been applied to the case of GBS electron linac using ELEGANT code choosing RFD phase 0° . The bunch length measurement relative error has been less than 0.2%. The bunch length virtual measurement relative error for $\varphi = 180^\circ$ ([15]) is smaller than the relative error for $\varphi = 0^\circ$. The comparison between simulation and theoretical results of vertical bunch centroid and divergence average at screen have been reported. Moreover, the goodness of the approximation in the evaluation of calibration factor by means of self-calibrate measurements has been showed. These plots has been carried out varying RFD phase between -30° and 30° , and -150° and 210° . The plots have been showed a good match between theoretical predictions and simulated data of vertical bunch centroid and divergence average both RFD phase range between -30° and 30° , and -150° and 210° . The maximum relative error between theoretical and approximated calibration factor is less than 0.07% in both RFD phase ranges. These results are preliminary steps for a metrological characterization of the bunch length measurement by means of a RFD.

References

- [1] "The White Book of ELI Nuclear Physics Bucharest-Magurele, Romania". In: *available on-line at <http://www.eli-np.ro/documents/ELI-NP-WhiteBook.pdf>* ().
- [2] L. Serafini et al. "Technical Design Report EuroGammaS proposal for the ELI-NP Gamma beam System". In: *arXiv preprint arXiv:1407.3669* (2014).
- [3] A. Bacci et al. "Electron Linac design to drive bright Compton back-scattering gamma-ray sources". In: *Journal of Applied Physics* 113.19 (2013), p. 194508.
- [4] A. Mostacci et al. "Chromatic effects in quadrupole scan emittance measurements". In: *Physical Review Special Topics - Accelerators and Beams* 15.8 (2012).
- [5] A. Cianchi et al. "Six-dimensional measurements of trains of high brightness electron bunches". In: *Physical Review Special Topics - Accelerators and Beams* 18.8 (2015).
- [6] D. Filippetto et al. "Phase space analysis of velocity bunched beams". In: *Physical Review Special Topics - Accelerators and Beams* 14.9 (2011).
- [7] G. Loew and O. H. Altenmueller. "Design and applications of RF separator structures at SLAC". In: *5th International Conference on High-Energy Accelerators, Frascati*. 1965, pp. 438–442.
- [8] P. Emma, J. Frisch, and P. Krejcik. "A Transverse RF deflecting structure for bunch length and phase space diagnostics". In: *LCLS Technical Note 12* (2000).
- [9] R. Akre, L. Bentson, P. Emma, and P. Krejcik. "Bunch length measurements using a transverse RF deflecting structure in the SLAC linac". In: *Proc. EPAC 2002 Conference*. 2002.
- [10] D. Alesini et al. "RF deflector design and measurements for the longitudinal and transverse phase space characterization at SPARC". In: *Nuclear Instruments and Methods in Physics Research Section A: Accelerators, Spectrometers, Detectors and Associated Equipment* 568.2 (2006), pp. 488–502.
- [11] D. Alesini and C. Vaccarezza. *Longitudinal and transverse phase space characterization*. Tech. rep. SPARCRF-03/003, INFN/LNF, Frascati, 2003.
- [12] A. Bacci et al. "Status of Thomson source at SPARC/PLASMONX". In: *Nuclear Instruments and Methods in Physics Research Section A: Accelerators, Spectrometers, Detectors and Associated Equipment* 608.1 (2009), S90–S93.
- [13] M. Borland. *Elegant: A flexible SDDS-compliant code for accelerator simulation*. Tech. rep. Argonne National Lab., IL (US), 2000.
- [14] M. Borland. "User's Manual for elegant". In: *available on-line at http://www.aps.anl.gov/Accelerator_Systems_Division/Accelerator_Operations_Physics/manuals/elegant_latest/elegant.pdf* ver. 29.1.0 (2016).
- [15] L. Sabato et al. "Metrological characterization of the bunch length measurement by means of a RF deflector at the ELI-NP Compton gamma source". paper MOPMB018, presented at IPAC'16, Busan, Korea, 2016.
- [16] A. Cianchi. "Observations and Diagnostics in High Brightness Beams". proceedings CAS, "Intensity Limitations in Particle Beams, CERN, Geneva, Switzerland, 2 - 11 November, 2015, available on-line at <http://cas.web.cern.ch/cas/Intensity-Limitations-2015/Lectures/Friday6/Cianchi.pdf>. 2015.
- [17] D. Alesini et al. "Sliced beam parameter measurements". In: *Proceedings of EPAC*. 2009.
- [18] H. Wiedemann et al. *Particle accelerator physics*. Vol. 314. Springer, 2007.
- [19] A. W. Chao, K. H. Mess, M. Tigner, and F. Zimmermann. *Handbook of accelerator physics and engineering*. World scientific, 2013.
- [20] K. Bongardt. *Calculation of the transfer matrix T in six dimensions for an rf-deflector element*. Tech. rep. 1981.